Journal of Sound and Vibration 329 (2010) 3744–3758

Contents lists available at ScienceDirect

Journal of Sound and Vibration

journal homepage: www.elsevier.com/locate/jsvi

A distributed-mass approach for dynamic analysis of Bernoulli–Euler plane frames

Hsiang-Chuan Tsai *

Department of Construction Engineering, National Taiwan University of Science and Technology, 43, Section 4, Keelong Road, P.O. Box 90-130, Taipei 106, Taiwan

ARTICLE INFO

Article history:
Received 8 October 2009
Received in revised form
9 March 2010
Accepted 10 March 2010
Handling Editor: S. Ilanko
Available online 20 April 2010

ABSTRACT

The exact dynamic analysis of plane frames should consider the effect of mass distribution in beam elements, which can be achieved by using the dynamic stiffness method. Solving for the natural frequencies and mode shapes from the dynamic stiffness matrix is a nonlinear eigenproblem. The Wittrick–Williams algorithm is a reliable tool to identify the natural frequencies. A deflated matrix method to determine the mode shapes is presented. The dynamic stiffness matrix may create some null modes in which the joints of beam elements have null deformation. Adding an interior node at the middle of beam elements can eliminate the null modes of flexural vibration, but does not eliminate the null modes of axial vibration. A force equilibrium approach to solve for the null modes of axial vibration is presented. Orthogonal conditions of vibration modes in the Bernoulli–Euler plane frames, which are required in solving the transient response, are theoretically derived. The decoupling process for the vibration modes of the same natural frequency is also presented.

1. Introduction

Vibration of a beam element can be modeled as a continuous-coordinate system and solved from the differential equation of motion and the related boundary conditions. Vibration of a plane frame, which is an assemblage of beam elements, is usually analyzed by a discrete-coordinate system in which the stiffness matrix is established through the static equilibrium equation of beam elements; the mass matrix may be formed either by lumping the mass at the structural joints, called the lumped-mass method, or from the static-deformed shape functions of beam elements, called the consistent-mass method. The solutions of the discrete models only approximate the actual dynamic behavior. Craig [1] compared the natural frequencies of a uniform cantilever beam from the exact continuous model and the two discrete models approximated by the lumped-mass method and the consistent-mass method, which revealed that the accuracy of the natural frequencies calculated by the discrete models deteriorates in the higher modes. The continuous-model approach utilized in the dynamic analysis of a single beam element is recognized to not be feasible for the dynamic analysis of plane frames because the necessary boundary conditions become unmanageable [2].

From the differential equation of beam vibration, the relationships between harmonic forces and displacements at the ends of a beam element can be exactly established. These relations are usually referred to as the dynamic stiffness matrix. The elements in the dynamic stiffness matrix are nonlinear functions, trigonometric and hyperbolic, of vibration frequency. By expanding the dynamic stiffness matrix in Taylor's series, Paz [3] demonstrated that the first term of the series, the zero

* Tel.: +886 2 27376581; fax: +886 2 27376606.
E-mail address: hctsai@mail.ntust.edu.tw

0022-460X/$ - see front matter © 2010 Elsevier Ltd. All rights reserved.
doi:10.1016/j.jsv.2010.03.013

power of frequency, is the static stiffness matrix, and the second term of the series, the second power of frequency, is the consistent mass matrix. After the dynamic stiffness matrices of beam elements are derived, the dynamic stiffness matrix of the whole frame can be assembled by exactly the same procedure used in the static matrix structural analysis. The historical development of using the dynamic stiffness matrix in structural dynamics has been highlighted by Akesson [4].

The dynamic stiffness matrix, which is frequency-dependent, can be directly employed in solving the steady-state response of the frames subjected to harmonic loadings. To solve the problems of transient response, the natural frequencies and mode shapes of the frames must be first calculated from the dynamic stiffness matrix. The calculation is usually referred to as a nonlinear eigenproblem and is different from the linear eigenproblem encountered in the dynamic analysis of discrete systems. Extending the Sturm sequence property of linear eigenproblems, the Wittrick–Williams algorithm [5,6] can count the number of vibration modes exceeded by a specified frequency from the dynamic stiffness matrix. This ensures that no natural frequencies are missed when using the bisection or other methods [7] to solve the zero determinant equation of the dynamic stiffness matrix.

The orthogonality of vibration modes is the required condition of using the vibration modes to solve the transient response of the frames. Although the derivation of orthogonal conditions for the vibration modes in discrete systems can be easily found in textbooks of structural dynamics [1,2], the publications on the orthogonality of vibration modes employed in the dynamic stiffness matrix are few and less rigorous [8]. The present paper derives the mode orthogonality conditions of the Bernoulli–Euler plane frame with distributed mass for the modes of different natural frequencies. Using the mode orthogonality, the equations of motion, in terms of structural joint deformation, can be transformed into the decoupled equations of motion in terms of vibration mode amplitudes. Not every vibration mode has distinct natural frequency. Sometimes several modes may have the same natural frequency, which are called the modes of repeated roots. The decoupling process for the modes of repeated roots is also derived in this paper.

There are several methods to solve the mode shapes from the dynamic stiffness matrix [9]. However, these methods have been shown not to be very stable [10]. A deflated matrix approach to solve the mode shapes from the dynamic stiffness matrix is proposed in the present paper, which is also extended to find the orthogonal mode shapes of the repeated-root modes.

In the vibration of frames considering the effect of distributed mass, a special set of vibration modes may occur in which the deformations at all frame joints are null but the deformations in beam elements are not null. This set of vibration modes is called the null modes here. The null mode shapes cannot be directly solved from the dynamic stiffness matrix. Dias and Alves [11] included the degrees of freedom at the joints of beam elements and the constants in the shape functions of beam elements in the eigenproblem, which can eliminate the null modes but has to pay the price of an increased matrix order. The null modes relating to flexural vibration can be easily removed by adding an interior node at the middle of beam elements [10]. For the null modes relating to axial vibration, adding the interior node cannot eliminate the null modes completely. An efficient approach by use of the force equilibrium is presented in this paper.

2. Dynamic stiffness matrices

The prismatic beam element shown in Fig. 1 has length L, cross-sectional area A, second moment of area I, Young's modulus E, and density ρ. When the beam is vibrating at a specific frequency ω, the axial displacement in the x direction, u, and the transverse displacement in the y direction, v, can be expressed as

$$u(x,t)=\chi(x)e^{i\omega t},\quad v(x,t)=\psi(x)e^{i\omega t} \tag{1}$$

in which χ is the axial shape function, ψ is the transverse shape function, and t is time variable. Dynamic equilibrium of the Bernoulli–Euler beam gives

$$\chi(x)=a_1\cos\alpha x+a_2\sin\alpha x \tag{2}$$

$$\psi(x)=b_1\cos\beta x+b_2\sin\beta x+b_3\cosh\beta x+b_4\sinh\beta x \tag{3}$$

with

$$\alpha=\omega\sqrt{(\rho A)/(EA)},\quad \beta=\sqrt[4]{(\rho A)/(EI)}\sqrt{\omega} \tag{4}$$

The relation between the constants a_i and the axial displacements at the beam ends, $\chi(0)$ and $\chi(L)$, can be solved from Eq. (2). The relation between the constants b_i and the transverse displacements and slopes at the beam ends, $\psi(0)$, $\psi'(0)$, $\psi(L)$ and $\psi'(L)$, can be solved from Eq. (3).

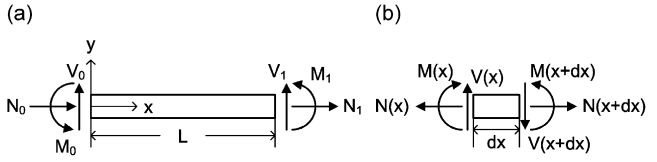

Fig. 1. Positive directions of force components in a beam element: (a) end forces and (b) internal forces.

The axial force N, bending moment M, and shear force V in the prismatic Bernoulli–Euler beam have the following relations with the axial and transverse displacements:

$$N(x)=EA\chi'(x),\quad M(x)=EI\psi''(x),\quad V(x)=EI\psi'''(x) \tag{5}$$

Let N_0, M_0, V_0, χ_0, ψ_0 and θ_0 denote the axial force, bending moment, shear force, axial displacement, transverse displacement and slope, respectively, at the beam end of $x=0$, and N_1, M_1, V_1, χ_1, ψ_1 and θ_1 be the corresponding quantities at the beam end of $x=L$. The positive directions of the end forces and internal forces are shown in Fig. 1, which give the relations

$$N_0=-N(0),\quad M_0=-M(0),\quad V_0=V(0),\quad \chi_0=\chi(0),\quad \psi_0=\psi(0),\quad \theta_0=\psi'(0) \tag{6}$$

$$N_1=N(L),\quad M_1=M(L),\quad V_1=-V(L),\quad \chi_1=\chi(L),\quad \psi_1=\psi(L),\quad \theta_1=\psi'(L) \tag{7}$$

Substituting Eqs. (2) and (3) into Eq. (5) and using the relations in Eqs. (6) and (7), the dynamic stiffness of the Bernoulli–Euler beam can be derived:

$$\begin{Bmatrix} N_0\\ V_0\\ M_0\\ N_1\\ V_1\\ M_1 \end{Bmatrix} = EI \begin{bmatrix} \frac{A\alpha}{I\tan\alpha L} & 0 & 0 & -\frac{A\alpha}{I\sin\alpha L} & 0 & 0\\ 0 & \frac{\beta^3B_1}{B_0} & \frac{\beta^2B_3}{B_0} & 0 & -\frac{\beta^3B_4}{B_0} & \frac{\beta^2B_6}{B_0}\\ 0 & \frac{\beta^2B_3}{B_0} & \frac{\beta B_2}{B_0} & 0 & -\frac{\beta^2B_6}{B_0} & \frac{\beta B_5}{B_0}\\ -\frac{A\alpha}{I\sin\alpha L} & 0 & 0 & \frac{A\alpha}{I\tan\alpha L} & 0 & 0\\ 0 & -\frac{\beta^3B_4}{B_0} & -\frac{\beta^2B_6}{B_0} & 0 & \frac{\beta^3B_1}{B_0} & -\frac{\beta^2B_3}{B_0}\\ 0 & \frac{\beta^2B_6}{B_0} & \frac{\beta B_5}{B_0} & 0 & -\frac{\beta^2B_3}{B_0} & \frac{\beta B_2}{B_0} \end{bmatrix} \begin{Bmatrix} \chi_0\\ \psi_0\\ \theta_0\\ \chi_1\\ \psi_1\\ \theta_1 \end{Bmatrix} \tag{8}$$

with $B_0=1-\cos\beta L\cosh\beta L$, $B_1=\sin\beta L\cosh\beta L+\cos\beta L\sinh\beta L$, $B_2=\sin\beta L\cosh\beta L-\cos\beta L\sinh\beta L$, $B_3=\sin\beta L\sinh\beta L$, $B_4=\sinh\beta L+\sin\beta L$, $B_5=\sinh\beta L-\sin\beta L$, $B_6=\cosh\beta L-\cos\beta L$

The plane frame shown in Fig. 2 is defined by a global coordinate system $(\overline{x},\overline{y})$. Let $\overline{u}_i$, $\overline{v}_i$ and $\overline{\theta}_i$ denote the displacements in the $\overline{x}$ and $\overline{y}$ directions and the rotation, respectively, at joint i. Let $\overline{X}_i$, $\overline{Y}_i$ and $\overline{M}_i$ denote the forces in the $\overline{x}$ and $\overline{y}$ directions and the moment, respectively, acting at the joint i of the element J. The total number of the unconstrained degrees of freedom in the joints of the frame is denoted as n_d.

The dynamic stiffness matrix in Eq. (8) can be transformed to the element stiffness matrix in the global coordinate system. The global stiffness matrices of all elements in the frame are then assembled to form the frame stiffness matrix $\mathbf{K}(\omega)$ by means of the direct stiffness method, which yields

$$\mathbf{K}(\omega)\mathbf{d}=\mathbf{0} \tag{9}$$

in which $\mathbf{K}(\omega)$ is a $n_d\times n_d$ matrix and is a function of frequency, and $\mathbf{d}$ is the displacement vector of the unconstrained degrees of freedom in the joints of the frame.

3. Orthogonality of mode shape functions

After the nth mode shape vector $\mathbf{d}_n$ of the frame is solved, the axial and transverse shape functions of element J in the nth mode, χ_{Jn} and ψ_{Jn}, respectively, can be derived from Eqs. (2) and (3). The equations of motion for element J vibrating in the nth mode with natural frequency ω_n are

$$-(EA)_J\frac{d^2\chi_{Jn}}{dx_J^2}-(\rho A)_J\omega_n^2\chi_{Jn}=0 \tag{10}$$

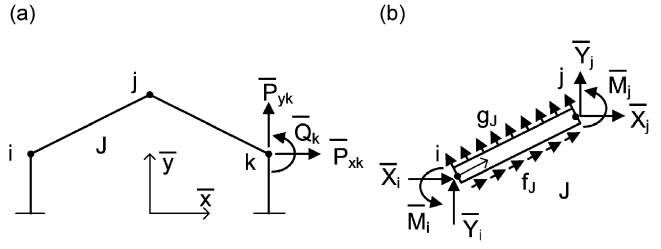

Fig. 2. External loads acting on a plane frame: (a) nodal loads and (b) element loads.

$$(EI)_J \frac{d^4\psi_{Jn}}{dx_J^4} - (\rho A)_J \omega_n^2 \psi_{Jn} = 0 \tag{11}$$

in which $(EA)_J$, $(EI)_J$, $(\rho A)_J$ and x_J are the axial stiffness, flexural stiffness, mass per unit length, and axial coordinate of element J, respectively. After multiplying Eqs. (10) and (11) by the axial and transverse shape functions of element J in the mth mode, respectively, and then integrating the summation of the two equations through the element length L_J, the summation of the integrations of all elements leads to

$$\sum_J \int_0^{L_J} \left\{ \psi_{Jm} \left[(EI)_J \psi_{Jn}^{IV} - (\rho A)_J \omega_n^2 \psi_{Jn} \right] - \chi_{Jm} \left[(EA)_J \chi_{Jn}'' + (\rho A)_J \omega_n^2 \chi_{Jn} \right] \right\} dx_J = 0 \tag{12}$$

which becomes, through integration by part,

$$\sum_J \int_0^{L_J} \{ (EI)_J \psi_{Jm}'' \psi_{Jn}'' + (EA)_J \chi_{Jm}' \chi_{Jn}' - \omega_n^2 (\rho A)_J (\psi_{Jm}\psi_{Jn} + \chi_{Jm}\chi_{Jn}) \} dx_J = \sum_J (-\psi_{Jm} V_{Jn} + \psi_{Jm}' M_{Jn} + \chi_{Jm} N_{Jn})|_0^{L_J} \tag{13}$$

The right side of Eq. (13) can be expressed in vector form by using the notation similar to Eqs. (6) and (7):

$$\sum_J (-\psi_{Jm} V_{Jn} + \psi_{Jm}' M_{Jn} + \chi_{Jm} N_{Jn})|_0^{L_J} = \sum_J \left(\begin{Bmatrix} (\chi_1)_{Jm} \\ (\psi_1)_{Jm} \\ (\theta_1)_{Jm} \end{Bmatrix}^T \begin{Bmatrix} (N_1)_{Jn} \\ (V_1)_{Jn} \\ (M_1)_{Jn} \end{Bmatrix} + \begin{Bmatrix} (\chi_0)_{Jm} \\ (\psi_0)_{Jm} \\ (\theta_0)_{Jm} \end{Bmatrix}^T \begin{Bmatrix} (N_0)_{Jn} \\ (V_0)_{Jn} \\ (M_0)_{Jn} \end{Bmatrix} \right) \tag{14}$$

The transformation between the element local coordinates and the frame global coordinates gives, with $\mathbf{T}$ being the transformation matrix:

$$\begin{Bmatrix} (\chi_0)_{Jm} \\ (\psi_0)_{Jm} \\ (\theta_0)_{Jm} \end{Bmatrix}^T \begin{Bmatrix} (N_0)_{Jn} \\ (V_0)_{Jn} \\ (M_0)_{Jn} \end{Bmatrix} = \begin{Bmatrix} (\overline{u}_i)_m \\ (\overline{v}_i)_m \\ (\overline{\theta}_i)_m \end{Bmatrix}^T \mathbf{T}^T \mathbf{T} \begin{Bmatrix} (\overline{X}_i)_{Jn} \\ (\overline{Y}_i)_{Jn} \\ (\overline{M}_i)_{Jn} \end{Bmatrix} = \begin{Bmatrix} (\overline{u}_i)_m \\ (\overline{v}_i)_m \\ (\overline{\theta}_i)_m \end{Bmatrix}^T \begin{Bmatrix} (\overline{X}_i)_{Jn} \\ (\overline{Y}_i)_{Jn} \\ (\overline{M}_i)_{Jn} \end{Bmatrix} \tag{15}$$

which means

$$\sum_J \left(\begin{Bmatrix} (\chi_1)_{Jm} \\ (\psi_1)_{Jm} \\ (\theta_1)_{Jm} \end{Bmatrix}^T \begin{Bmatrix} (N_1)_{Jn} \\ (V_1)_{Jn} \\ (M_1)_{Jn} \end{Bmatrix} + \begin{Bmatrix} (\chi_0)_{Jm} \\ (\psi_0)_{Jm} \\ (\theta_0)_{Jm} \end{Bmatrix}^T \begin{Bmatrix} (N_0)_{Jn} \\ (V_0)_{Jn} \\ (M_0)_{Jn} \end{Bmatrix} \right) = \sum_i \left(\begin{Bmatrix} (\overline{u}_i)_m \\ (\overline{v}_i)_m \\ (\overline{\theta}_i)_m \end{Bmatrix}^T \sum_{J \in i} \begin{Bmatrix} (\overline{X}_i)_{Jn} \\ (\overline{Y}_i)_{Jn} \\ (\overline{M}_i)_{Jn} \end{Bmatrix} \right) = 0 \tag{16}$$

where the element $J \in i$ means the element connecting to node i. Without any external force acting at node i, the internal end forces of all the elements connecting to node i are in balance, which leads to zero in the above equation. Using Eq. (16), Eq. (13) becomes

$$\sum_J \int_0^{L_J} \left\{ (EI)_J \psi_{Jm}'' \psi_{Jn}'' + (EA)_J \chi_{Jm}' \chi_{Jn}' - \omega_n^2 (\rho A)_J (\psi_{Jm}\psi_{Jn} + \chi_{Jm}\chi_{Jn}) \right\} dx_J = 0 \tag{17}$$

Multiplying the equations of axial and transverse motions of element J vibrating in the mth mode by the axial and transverse shape functions of element J in the nth mode, respectively, the following equation can be established:

$$\sum_J \int_0^{L_J} \left\{ \psi_{Jn} \left[(EI)_J \psi_{Jm}^{IV} - (\rho A)_J \omega_m^2 \psi_{Jm} \right] - \chi_{Jn} \left[(EA)_J \chi_{Jm}'' + (\rho A)_J \omega_m^2 \chi_{Jm} \right] \right\} dx_J = 0 \tag{18}$$

Using the similar procedure described in the last paragraph, the following equation is derived:

$$\sum_J \int_0^{L_J} \left\{ (EI)_J \psi_{Jn}'' \psi_{Jm}'' + (EA)_J \chi_{Jn}' \chi_{Jm}' - \omega_m^2 (\rho A)_J (\psi_{Jn}\psi_{Jm} + \chi_{Jn}\chi_{Jm}) \right\} dx_J = 0 \tag{19}$$

Subtracting Eq. (17) from Eq. (19) gives the following mass-related orthogonal equation of mode shapes:

$$\sum_J (\rho A)_J \int_0^{L_J} (\psi_{Jm}\psi_{Jn} + \chi_{Jm}\chi_{Jn}) dx_J = 0 \quad \text{for } \omega_m \neq \omega_n \tag{20}$$

The stiffness-related orthogonal equation is derived by substituting Eq. (20) into Eq. (17):

$$\sum_J \int_0^{L_J} \{ (EI)_J \psi_{Jm}'' \psi_{Jn}'' + (EA)_J \chi_{Jm}' \chi_{Jn}' \} dx_J = 0 \quad \text{for } \omega_m \neq \omega_n \tag{21}$$

Bringing in Eq. (20), Eq. (12) gives another form of the stiffness-related orthogonal equation:

$$\sum_J \int_0^{L_J} \{ (EI)_J \psi_{Jm} \psi_{Jn}^{IV} - (EA)_J \chi_{Jm} \chi_{Jn}'' \} dx_J = 0 \quad \text{for } \omega_m \neq \omega_n \tag{22}$$

By setting $m=n$ in Eq. (12), the natural frequency and mode shape has the relation as

$$\sum_J \int_0^{L_J} \left[(EI)_J \psi_{Jn} \psi_{Jn}^{IV} - (EA)_J \chi_{Jn} \chi_{Jn}''\right] dx_J = \omega_n^2 \sum_J \int_0^{L_J} (\rho A)_J \left(\psi_{Jn}^2 + \chi_{Jn}^2\right) dx_J \tag{23}$$

4. Equations of motion for generalized coordinates

The damping property of the frame can be described through two parameters, ζ and η, where ζ is the stiffness-related viscous damping ratio and η is the mass-related viscous damping ratio. When element J is subjected to distributed loads in the axial and transverse directions, denoted as f_J and g_J, respectively, as shown in Fig. 2, the equations of motion for element J with viscous damping are

$$-(EA)_J \left(\frac{\partial^2 u_J}{\partial x_J^2} + \zeta \frac{\partial^3 u_J}{\partial x_J^2 \partial t}\right) + (\rho A)_J \left(\frac{\partial^2 u_J}{\partial t^2} + \eta \frac{\partial u_J}{\partial t}\right) = f_J(x_J,t) \tag{24}$$

$$(EI)_J \left(\frac{\partial^4 v_J}{\partial x_J^4} + \zeta \frac{\partial^5 v_J}{\partial x_J^4 \partial t}\right) + (\rho A)_J \left(\frac{\partial^2 v_J}{\partial t^2} + \eta \frac{\partial v_J}{\partial t}\right) = g_J(x_J,t) \tag{25}$$

The displacements of force vibration can be expressed as the linear combination of all mode shapes

$$u_J(x_J,t) = \sum_{k=1}^{\infty} \chi_{Jk}(x_J) q_k(t) \tag{26}$$

$$v_J(x_J,t) = \sum_{k=1}^{\infty} \psi_{Jk}(x_J) q_k(t) \tag{27}$$

in which the generalized coordinate q_k represents the amplitude of the kth mode. If the frame has a virtual displacement as the nth mode shape, the theory of virtual work gives

$$\sum_J \int_0^{L_J} \psi_{Jn} \sum_{k=1}^{\infty} \left[(EI)_J \psi_{Jk}^{IV} (q_k + \zeta \dot{q}_k) + (\rho A)_J \psi_{Jk} (\ddot{q}_k + \eta \dot{q}_k)\right] dx_J + \sum_J \int_0^{L_J} \chi_{Jn} \sum_{k=1}^{\infty} \left[-(EA)_J \chi_{Jk}''(q_k + \zeta \dot{q}_k) + (\rho A)_J \chi_{Jk} (\ddot{q}_k + \eta \dot{q}_k)\right] dx_J$$

$$= \sum_J \int_0^{L_J} (\psi_{Jn} g_J + \chi_{Jn} f_J)\, dx_J + \sum_i \left[(\overline{u}_i)_n \overline{P}_{xi} + (\overline{v}_i)_n \overline{P}_{yi} + (\overline{\theta}_i)_n \overline{Q}_i\right] \tag{28}$$

in which $\overline{P}_{xi}$, $\overline{P}_{yi}$ and $\overline{Q}_i$ are the horizontal force, vertical force and moment, respectively, externally acting at node i as shown in Fig. 2, and $(\overline{u}_i)_n$, $(\overline{v}_i)_n$ and $(\overline{\theta}_i)_n$ are the displacements in the $\overline{x}$ and $\overline{y}$ directions and the rotation at node i, respectively, of the nth mode shape.

If the nth mode is single root, i.e. $\omega_n \neq \omega_k$ for $n \neq k$, Eq. (28) can be decoupled by using the orthogonal conditions in Eqs. (20) and (22):

$$\left\{\sum_J \int_0^{L_J} \left[(EI)_J \psi_{Jn} \psi_{Jn}^{IV} - (EA)_J \chi_{Jn} \chi_{Jn}''\right] dx_J\right\} (q_n + \zeta \dot{q}_n) + \left\{\sum_J \int_0^{L_J} (\rho A)_J (\psi_{Jn}^2 + \chi_{Jn}^2)\, dx_J\right\} (\ddot{q}_n + \eta \dot{q}_n) = p_n(t) \tag{29}$$

in which p_n is the generalized force of the nth mode, defined as

$$p_n(t) = \sum_J \int_0^{L_J} (\psi_{Jn} g_J + \chi_{Jn} f_J)\, dx_J + \sum_i \left[(\overline{u}_i)_n \overline{P}_{xi} + (\overline{v}_i)_n \overline{P}_{yi} + (\overline{\theta}_i)_n \overline{Q}_i\right] \tag{30}$$

By using Eq. (23), Eq. (29) can be simplified as

$$\ddot{q}_n + (\eta + \omega_n^2 \zeta) \dot{q}_n + \omega_n^2 q_n = \frac{p_n(t)}{m_{nn}} \tag{31}$$

in which m_{nn} is the generalized mass of the nth mode, defined as

$$m_{nn} = \sum_J \int_0^{L_J} (\rho A)_J (\psi_{Jn}^2 + \chi_{Jn}^2)\, dx_J \tag{32}$$

The solution of the mode amplitude in Eq. (31) is a Duhamel integral.

5. Vibration modes of repeated roots

The equation of motion in Eq. (31) is derived for the modes of single root. For the modes of repeated roots, Eq. (28) cannot be decoupled. Let the modes between the cth mode and the dth mode be the repeated-root mode with the same

frequency ω_c. Using the orthogonal conditions in Eqs. (20) and (22), Eq. (28) gives, for $c \le n \le d$,

$$\sum_J \int_0^{L_J} \psi_{Jn} \sum_{k=c}^{d} \left[(EI)_J \psi_{Jk}^{IV} (q_k + \zeta \dot{q}_k) + (\rho A)_J \psi_{Jk} (\ddot{q}_k + \eta \dot{q}_k) \right] dx_J + \sum_J \int_0^{L_J} \chi_{Jn} \sum_{k=c}^{d} \left[-(EA)_J \chi_{Jk}'' (q_k + \zeta \dot{q}_k) + (\rho A)_J \chi_{Jk} (\ddot{q}_k + \eta \dot{q}_k) \right] dx_J = p_n(t) \tag{33}$$

which can be rearranged as

$$\sum_{k=c}^{d} \sum_J \int_0^{L_J} \left[(EI)_J \psi_{Jn} \psi_{Jk}^{IV} - (EA)_J \chi_{Jn} \chi_{Jk}'' \right] dx_J (q_k + \zeta \dot{q}_k) + \sum_{k=c}^{d} \sum_J (\rho A)_J \int_0^{L_J} (\psi_{Jn} \psi_{Jk} + \chi_{Jn} \chi_{Jk}) \, dx_J (\ddot{q}_k + \eta \dot{q}_k) = p_n(t) \tag{34}$$

Eq. (12) can be expressed as

$$\sum_J \int_0^{L_J} \left[(EI)_J \psi_{Jn} \psi_{Jk}^{IV} - (EA)_J \chi_{Jn} \chi_{Jk}'' \right] dx_J = \omega_k^2 \sum_J (\rho A)_J \int_0^{L_J} \left[\psi_{Jn} \psi_{Jk} + \chi_{Jn} \chi_{Jk} \right] dx_J \tag{35}$$

The substitution of Eq. (35) into Eq. (34) yields, for $c \le n \le d$:

$$\sum_{k=c}^{d} \sum_J (\rho A)_J \int_0^{L_J} (\psi_{Jn} \psi_{Jk} + \chi_{Jn} \chi_{Jk}) \, dx_J [\ddot{q}_k + (\eta + \omega_c^2 \zeta) \dot{q}_k + \omega_c^2 q_k] = p_n(t) \tag{36}$$

which can be expressed in the matrix form

$$\begin{bmatrix} m_{cc} & \cdots & m_{cd} \\ \vdots & \ddots & \vdots \\ m_{dc} & \cdots & m_{dd} \end{bmatrix} \begin{Bmatrix} \ddot{q}_c + (\eta + \omega_c^2 \zeta) \dot{q}_c + \omega_c^2 q_c \\ \vdots \\ \ddot{q}_d + (\eta + \omega_c^2 \zeta) \dot{q}_d + \omega_c^2 q_d \end{Bmatrix} = \begin{Bmatrix} p_c(t) \\ \vdots \\ p_d(t) \end{Bmatrix} \tag{37}$$

with the generalized mass term being

$$m_{nk} = \sum_J \int_0^{L_J} (\rho A)_J (\psi_{Jn} \psi_{Jk} + \chi_{Jn} \chi_{Jk}) \, dx_J \tag{38}$$

The equations of motion for the repeated-root generalized coordinates can be decoupled as

$$\begin{Bmatrix} \ddot{q}_c + (\eta + \omega_c^2 \zeta) \dot{q}_c + \omega_c^2 q_c \\ \vdots \\ \ddot{q}_d + (\eta + \omega_c^2 \zeta) \dot{q}_d + \omega_c^2 q_d \end{Bmatrix} = \begin{bmatrix} m_{cc} & \cdots & m_{cd} \\ \vdots & \ddots & \vdots \\ m_{dc} & \cdots & m_{dd} \end{bmatrix}^{-1} \begin{Bmatrix} p_c(t) \\ \vdots \\ p_d(t) \end{Bmatrix} \tag{39}$$

6. Solution of natural frequencies

The dynamic stiffness matrix of beam elements has a characteristic of being infinite at particular frequencies. The flexural dynamic stiffness in Eq. (8) becomes infinite when

$$B_0(\omega) = 1 - \cos \beta L \cosh \beta L = 0 \tag{40}$$

For a single beam having both ends clamped, i.e., $\psi(0) = \psi(L) = \psi'(0) = \psi'(L) = 0$, to have a nontrivial shape function $\psi(x)$ defined in Eq. (3), Eq. (40) must be fulfilled. In other words, the frequencies solved from Eq. (40) are the natural frequencies of flexural vibration in the beam element with both ends clamped, which will be called flexural poles here. The nth solution of Eq. (40), ω_{bn}, can be solved approximately by

$$\cos \beta L = 1/\cosh \beta L \approx 0 \quad \text{as } \beta L \gg 1 \tag{41}$$

which gives

$$\omega_{bn} \approx \left(n + \frac{1}{2} \right)^2 \frac{\pi^2}{L^2} \sqrt{\frac{EI}{\rho A}} \tag{42}$$

Similarly, the axial dynamic stiffness in Eq. (8) becomes infinite when

$$A_0(\omega) = \sin \alpha L = 0 \tag{43}$$

For a single beam having both ends fixed in the axial direction, i.e., $\chi(0) = \chi(L) = 0$, the shape function in Eq. (2) becomes

$$\chi(x) = a_2 \sin \alpha x \tag{44}$$

To have a nontrivial shape function, Eq. (43) must be fulfilled. In other words, the frequencies solved from Eq. (43) are the natural frequencies of axial vibration in the beam element without axial displacement at ends, which will be called axial

poles here. The nth solution of Eq. (43), ω_{an}, is

$$\omega_{an} = n\frac{\pi}{L}\sqrt{\frac{EA}{\rho A}} \tag{45}$$

The difficulty in finding the natural frequencies of frames in Eq. (9) arises from the existence of element poles. This can be overcome by using the Wittrick–Williams algorithm [5,6]. The algorithm states that $n_f(\omega)$, the total number of natural frequencies in a frame below a specific frequency ω, is given by

$$n_f(\omega) = n_p(\omega) + s\{\mathbf{K}(\omega)\} \tag{46}$$

where $n_p(\omega)$ is the total number of axial and flexural poles in all elements of the frame below the frequency ω; $s\{\mathbf{K}(\omega)\}$, the sign count of $\mathbf{K}(\omega)$, is the number of negative pivots in the diagonal matrix of pivots $\mathbf{D}$ after $\mathbf{K}(\omega)$ is factorized as

$$\mathbf{K}(\omega) = \mathbf{L}\mathbf{D}\mathbf{L}^T \tag{47}$$

in which $\mathbf{L}$ is a lower triangular matrix with all diagonal elements being unity.

By means of the bisection search method or other efficient methods [7], the natural frequencies of the frame can be numerically solved from the determinant of the frame dynamic stiffness matrix

$$\det \mathbf{K}(\omega) = \prod_{i=1}^{n_d} D_{ii} = 0 \tag{48}$$

where D_{ii} is the ith diagonal element in the pivot matrix $\mathbf{D}$, in cooperation with Eq. (46) which can guarantee no natural frequency being missed.

When searching the natural frequencies, it is usually necessary to find the number of vibration modes within a frequency interval. If the most poles in every element of the frame are a flexural pole and a axial pole between the lower frequency bound ω_l and the upper frequency bound ω_u, the Wittrick–Williams algorithm in Eq. (46) can be revised as

$$n_f(\omega_u) - n_f(\omega_l) = \operatorname{sgn} A_0(\omega_l,\omega_u) + \operatorname{sgn} B_0(\omega_l,\omega_u) + s\{\mathbf{K}(\omega_u)\} - s\{\mathbf{K}(\omega_l)\} \tag{49}$$

where $\operatorname{sgn} A_0(\omega_l,\omega_u)$ is the total number of elements in which the signs of the functions $A_0(\omega_l)$ and $A_0(\omega_u)$ are different, from + to − or from − to +, and $\operatorname{sgn} B_0(\omega_l,\omega_u)$ is the total number of elements in which the signs of the functions $B_0(\omega_l)$ and $B_0(\omega_u)$ are different.

The frequency difference between the n+1th and nth flexural poles of a beam element is, from Eq. (42),

$$\omega_{bn+1} - \omega_{bn} \approx 2(n+1)\frac{\pi^2}{L^2}\sqrt{\frac{EI}{\rho A}} \tag{50}$$

The frequency difference between the n+1th and nth axial poles of a beam element is, from Eq. (45),

$$\omega_{an+1} - \omega_{an} = \frac{\pi}{L}\sqrt{\frac{EA}{\rho A}} \tag{51}$$

If all the beam elements in the frame have the same section properties and same length, and the lower frequency bound ω_l is

$$\omega_l > \omega_{bn} \approx \left(n+\frac{1}{2}\right)^2\frac{\pi^2}{L^2}\sqrt{\frac{EI}{\rho A}} \tag{52}$$

the applicable frequency interval for Eq. (49) can be set by

$$\omega_u - \omega_l < \min\left\{2n\frac{\pi^2}{L^2}\sqrt{\frac{EI}{\rho A}}, \frac{\pi}{L}\sqrt{\frac{EA}{\rho A}}\right\} \tag{53}$$

If some beam elements in the frame have different section properties or different lengths, the applicable frequency interval for Eq. (49) in any frequency range can be made easier, but more conservative, by

$$\omega_u - \omega_l < \min_J\left\{2\frac{\pi^2}{L_J^2}\sqrt{\frac{(EI)_J}{(\rho A)_J}}, \frac{\pi}{L_J}\sqrt{\frac{(EA)_J}{(\rho A)_J}}\right\} \tag{54}$$

The approximate flexural poles solved from Eq. (41) may possess a larger error in the lower frequency. The exact solutions of the first two flexural poles are

$$\omega_{b1} = 22.3733\frac{1}{L^2}\sqrt{\frac{EI}{\rho A}} > (1.5)^2\frac{\pi^2}{L^2}\sqrt{\frac{EI}{\rho A}} = 22.2066\frac{1}{L^2}\sqrt{\frac{EI}{\rho A}}$$

$$\omega_{b2} = 61.6728\frac{1}{L^2}\sqrt{\frac{EI}{\rho A}} < (2.5)^2\frac{\pi^2}{L^2}\sqrt{\frac{EI}{\rho A}} = 61.6850\frac{1}{L^2}\sqrt{\frac{EI}{\rho A}}$$

The difference between the two poles is

$$\omega_{b2}-\omega_{b1}=39.2995\frac{1}{L^2}\sqrt{\frac{EI}{\rho A}}>2\frac{\pi^2}{L^2}\sqrt{\frac{EI}{\rho A}}=19.7392\frac{1}{L^2}\sqrt{\frac{EI}{\rho A}}$$

which means that the frequency interval in Eq. (54) is still applicable.

7. Solution of mode shape vectors

The natural frequency of the nth mode, ω_n, and the corresponding mode shape vector, $\mathbf{d}_n$, have the relation, from Eq. (9),

$$\mathbf{K}(\omega_n)\mathbf{d}_n=\mathbf{0} \tag{55}$$

Theoretically, $\mathbf{K}(\omega_n)$ is singular. Numerically, even if $\mathbf{K}(\omega_n)$ is not singular, $\mathbf{K}(\omega_n)$ is still ill-conditioned. The mode shape vector $\mathbf{d}_n$ can be calculated through the deflated matrix approach. Let $\overline{\mathbf{K}}_l(\omega_n)$ be the $(n_d-1)\times(n_d-1)$ matrix deflated by eliminating the lth row and lth column of $\mathbf{K}(\omega_n)$. The vector $\overline{\mathbf{d}}_l$, which has (n_d-1) dimensions, can be solved from

$$\overline{\mathbf{K}}_l(\omega_n)\overline{\mathbf{d}}_l=-\overline{\mathbf{c}}_l \tag{56}$$

where $\overline{\mathbf{c}}_l$, a vector of (n_d-1) dimensions, is the lth column of $\mathbf{K}(\omega_n)$ with the lth element removed. The mode shape vector $\mathbf{d}_n$ is obtained by expanding the vector $\overline{\mathbf{d}}_l$ as

$$\mathbf{d}_n=[\overline{d}_1\ \ \overline{d}_2\ \ \cdots\ \ \overline{d}_{l-1}\ \ 1\ \ \overline{d}_l\ \ \cdots\ \ \overline{d}_{n_d-1}]^T \tag{57}$$

where $\overline{d}_i$ is the ith element in the vector $\overline{\mathbf{d}}_l$.

One good choice of the deflated position l is the location where the absolute value of the pivot is the minimum in the pivot matrix $\mathbf{D}$ defined in Eq. (47). The accuracy of the calculated mode shape vector $\mathbf{d}_n$ can be checked by the residual vector $\mathbf{r}$ defined as

$$\mathbf{r}=\mathbf{K}(\omega_n)\mathbf{d}_n \tag{58}$$

If the norm of the residual vector is too large, select another deflated location l.

For the modes having n_r repeated roots, the space of the corresponding mode shape vectors is spanned by n_r orthogonal vectors. The deflated matrix approach in Eq. (56) can be used to find n_r independent vectors. The process of Gram–Schmidt orthogonalization is then applied to generate n_r orthogonal mode shape vectors which have $\mathbf{d}_n^T\mathbf{d}_k=0$ for $n\neq k$. These mode shape vectors have to be checked by Eq. (58) to guarantee low residual. There are many sets of orthogonal vectors that span the vector space of the modes having repeated roots. For any set of orthogonal vectors solved through the Gram–Schmidt process, the values of m_{nk} in Eq. (38) are usually negligible for $n\neq k$ and the equations in Eq. (37) are decoupled for the same frequency but different orthogonal mode shapes.

It should be noted that the deflated matrix approach is different from the P_z method of Ref. [9]. In the P_z method, the elements $\overline{d}_l$ to $\overline{d}_{n_d-1}$ are set to zero, and only the elements $\overline{d}_l$ to $\overline{d}_{l-1}$ are solved in Eq. (56).

8. Solution of null modes

There is one type of vibration modes of which the natural frequency is also the axial or flexural poles of some beam elements in the frame. This type of vibration modes is called null modes here, because the corresponding mode shape vector in Eq. (55) is null, $\mathbf{d}_n=\mathbf{0}$. Although the determinant of the frame dynamic stiffness matrix becomes infinite at the natural frequency of null modes, the Wittrick–Williams algorithm is still available to find null modes and solve the corresponding natural frequencies. The problem of null modes arises from failing to find the correct mode shape functions for the beam elements owning the poles. For the flexural poles, the shape function in Eq. (3) is not null, but the constants b_i cannot be determined by the null deformations at the ends of beam elements. Similarly, for the axial poles, the shape function in Eq. (2) is not null, but the constants a_i cannot be determined by the null deformations at the ends of beam elements. Numerically, the mode shape vectors of null modes solved by the deflated matrix approach described above may have very high residual, which can create wrong shape functions in the beam elements.

For the frame possessing the null modes of flexural poles, these null modes can be eliminated by adding an interior node at the middle of the beam elements owning the flexural poles [10]. The frequencies of flexural poles are the series of ω_{bn} shown in Eq. (42). Added by an interior node, the beam element is divided into two sub elements with the length $L=L^{(1)}+L^{(2)}$. The frequencies of flexural poles in the two sub elements are

$$\omega_{bn}^{(1)}\approx\left(n^{(1)}+\frac{1}{2}\right)^2\frac{\pi^2}{L^{(1)^2}}\sqrt{\frac{EI}{\rho A}};\quad \omega_{bn}^{(2)}\approx\left(n^{(2)}+\frac{1}{2}\right)^2\frac{\pi^2}{L^{(2)^2}}\sqrt{\frac{EI}{\rho A}} \tag{59}$$

To have $\omega_{bn}=\omega_{bn}^{(1)}=\omega_{bn}^{(2)}$, it must be

$$\frac{(n+1/2)^2}{L^2}=\frac{(n^{(1)}+1/2)^2}{L^{(1)^2}}=\frac{(n^{(2)}+1/2)^2}{L^{(2)^2}} \tag{60}$$

or

$$n^{(1)}=\left(n+\frac{1}{2}\right)\frac{L^{(1)}}{L}-\frac{1}{2};\quad n^{(2)}=\left(n+\frac{1}{2}\right)\frac{L^{(2)}}{L}-\frac{1}{2} \tag{61}$$

If $L^{(1)}=L^{(2)}=L/2$, it is impossible to find an integer value of $n^{(1)}$ or $n^{(2)}$ from any positive integer n. In other words, the frequencies of flexural poles in the sub elements will never coincide with ω_{bn} after adding an interior node at the middle of the beam elements. Therefore, the vibration mode of the frame which has the natural frequency ω_{bn} is no longer a null mode. However, if $L^{(1)}=L/3$ that yields $n^{(1)}=(n-1)/3$, the natural frequency ω_{bn} has a flexural pole in the first sub element when $n=4,7,10,\ldots$, and the frame still has null modes.

For the frame possessing the null modes of axial poles, the frequencies of axial poles are the series of ω_{an} shown in Eq. (45). After adding an interior node to the beam element of axial pole, the frequencies of axial poles in the two sub elements are

$$\omega_{an}^{(1)}=n^{(1)}\frac{\pi}{L^{(1)}}\sqrt{\frac{EA}{\rho A}};\quad \omega_{an}^{(2)}=n^{(2)}\frac{\pi}{L^{(2)}}\sqrt{\frac{EA}{\rho A}} \tag{62}$$

To have $\omega_{an}=\omega_{an}^{(1)}=\omega_{an}^{(2)}$, it must be

$$\frac{n}{L}=\frac{n^{(1)}}{L^{(1)}}=\frac{n^{(2)}}{L^{(2)}} \tag{63}$$

For any specific values of $L^{(1)}/L$, it is always possible to find some integer values of n that can generate integer values of $n^{(1)}$ or $n^{(2)}$. In other words, it is always possible to find some frequencies in the series of ω_{an} to coincide with axial poles in the sub elements. Therefore, adding an interior node to beam elements is unable to get rid of null mode of axial poles.

In the null modes of axial poles with frequency ω_{an}, the axial force in the ith beam element possessing axial pole has the form, derived from Eqs. (5) and (44),

$$N(x)=a_2EA\alpha\cos\alpha x=e_i\cos\alpha x \tag{64}$$

with $e_i=a_2EA\alpha$ being the magnitude of axial force in the ith axial-pole element. The axial forces acting at the ends of the ith axial-pole element become

$$N_0=-N(0)=-e_i;\quad N_1=N(L)=e_i\cos\alpha L=(-1)^n e_i \tag{65}$$

where $\cos\alpha L=(-1)^n$ because the corresponding frequency is ω_{an} defined in Eq. (45). In terms of the magnitude of axial force, the shape function in Eq. (44) becomes

$$\chi(x)=\frac{e_i}{EA\alpha}\sin\alpha x \tag{66}$$

In the null modes, the displacement vector $\mathbf{d}$ cannot be used as variables because it is null. Instead, the magnitudes of axial force in the beam elements possessing axial pole can be chosen as variables. If the null mode has n_e beam elements possessing axial pole in the frame, the axial-force vector $\mathbf{e}$ is a n_e-dimensional vector formed by elements e_i. After using Eq. (65) to calculate the end forces of all beam elements possessing axial pole, force equilibriums on all n_d unconstrained degrees of freedom in the frame lead to

$$\mathbf{Fe}=\mathbf{0} \tag{67}$$

where $\mathbf{F}$ is a $n_d\times n_e$ rectangular matrix. Allowing row and column exchanges, the forward Gaussian elimination can decompose Eq. (67) into

$$[\mathbf{U}\ \mathbf{V}]\bar{\mathbf{e}}=\mathbf{0} \tag{68}$$

where $\mathbf{U}$ is a $n_s\times n_s$ upper triangular matrix with all diagonal elements being nonzero, and $\mathbf{V}$ is a $n_s\times n_r$ matrix with n_r being the number of repeated roots in the null mode and $n_s=n_e-n_r$. If the null mode is single root, then $n_r=1$. The n_e-dimensional vector $\bar{\mathbf{e}}$ is the axial-force vector, but may have a different e_i sequence from the vector $\mathbf{e}$ because of column exchanges. The backward substitution on the matrix $\mathbf{U}$ yields

$$\mathbf{E}=-\mathbf{U}^{-1}\mathbf{V} \tag{69}$$

where $\mathbf{E}$, a $n_s\times n_r$ matrix, can be expanded as

$$\bar{\mathbf{E}}=\begin{bmatrix}\mathbf{E}\\ \mathbf{I}\end{bmatrix} \tag{70}$$

where $\mathbf{I}$ is the $n_r\times n_r$ unit matrix, and $\bar{\mathbf{E}}$ is the $n_e\times n_r$ matrix in which each column is the axial-force vector of each axial-pole root corresponding to the vector $\bar{\mathbf{e}}$. Then, the mode shape functions in the beam elements possessing axial pole can be calculated from Eq. (66).

Although the null modes of flexural poles may be solved by a similar procedure described in the last paragraph, adding an interior node at the middle of the beam elements as described before seems to be the easier way to get rid of the null modes of flexural poles.

9. Numerical examples

9.1. Example 1

The cross frame shown in Fig. 3(a) consists of four prismatic beams with 4 m length. Every beam has the same properties of $E=10^9\,\mathrm{N/m^2}$, $\rho=10^3\,\mathrm{kg/m^3}$, $A=10^{-2}\,\mathrm{m^2}$ and $I=10^{-5}\,\mathrm{m^4}$. To prevent the null modes of flexural poles, a node is added to the middle of each beam. Natural frequencies and mode shapes of the first eight modes are shown in Fig. 4. Modes 2 and 3 are the double-roots modes which have the same natural frequency and orthogonal mode shapes. In these two modes, the center joint of the cross frame does not rotate but has vertical and horizontal, respectively, translations. The corresponding generalized mass terms defined in Eq. (38) are $m_{22}=1.0$, $m_{23}=1.985\times10^{-23}$, $m_{33}=1.0$. The off-diagonal term

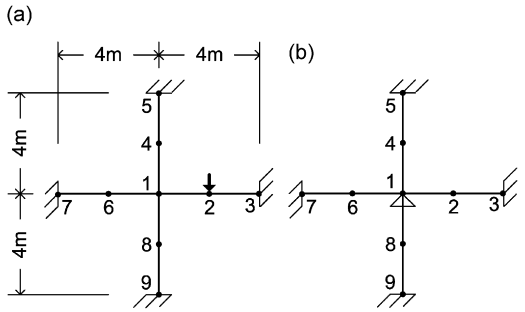

Fig. 3. Cross frames in example 1: (a) without hinge and (b) with hinge.

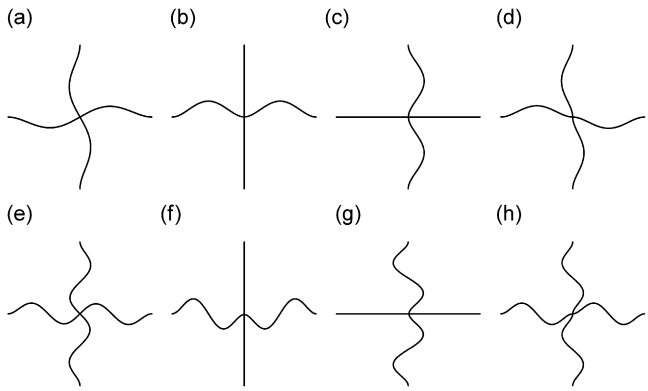

Fig. 4. The first eight modes in cross frame without hinge: (a) mode 1 (4.850 Hz); (b) mode 2 (7.018 Hz); (c) mode 3 (7.018 Hz); (d) mode 4 (7.038 Hz); (e) mode 5 (15.72 Hz); (f) mode 6 (19.23 Hz); (g) mode 7 (19.23 Hz) and (h) mode 8 (19.40 Hz).

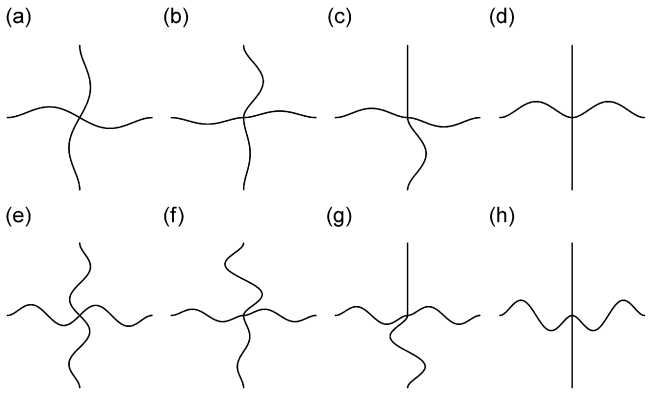

Fig. 5. The first eight modes in cross frame with hinge: (a) mode 1 (4.850 Hz); (b) mode 2 (7.038 Hz); (c) mode 3 (7.038 Hz); (d) mode 4 (7.038 Hz); (e) mode 5 (15.72 Hz); (f) mode 6 (19.40 Hz); (g) mode 7 (19.40 Hz) and (h) mode 8 (19.40 Hz).

m_{23} is very small. In mode 4, the center joint does not rotate and translate, so that its natural frequency is equal to ω_{b1}, the first flexural pole in Eq. (40) with L=4 m. Similarly, modes 6 and 7 are double-roots modes and mode 8 has natural frequency equal to ω_{b2}, the second flexural pole.

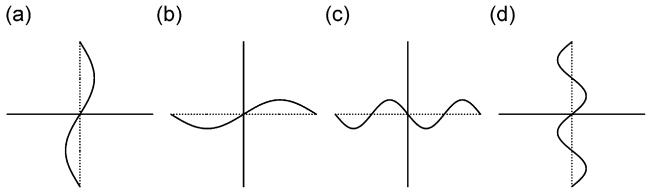

Fig. 6. Axial deformations of null modes of axial poles in cross frame without hinge: (a) mode 24 (125 Hz); (b) mode 25 (125 Hz); (c) mode 39 (250 Hz) and (d) mode 40 (250 Hz).

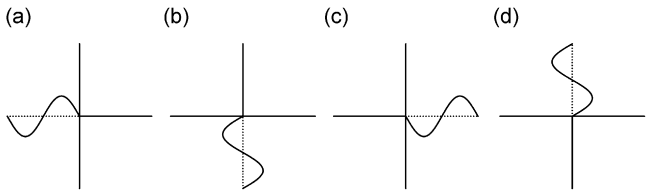

Fig. 7. Axial deformations of null modes of axial poles in cross frame with hinge: (a) mode 37 (250 Hz); (b) mode 38 (250 Hz); (c) mode 39 (250 Hz) and (d) mode 40 (250 Hz).

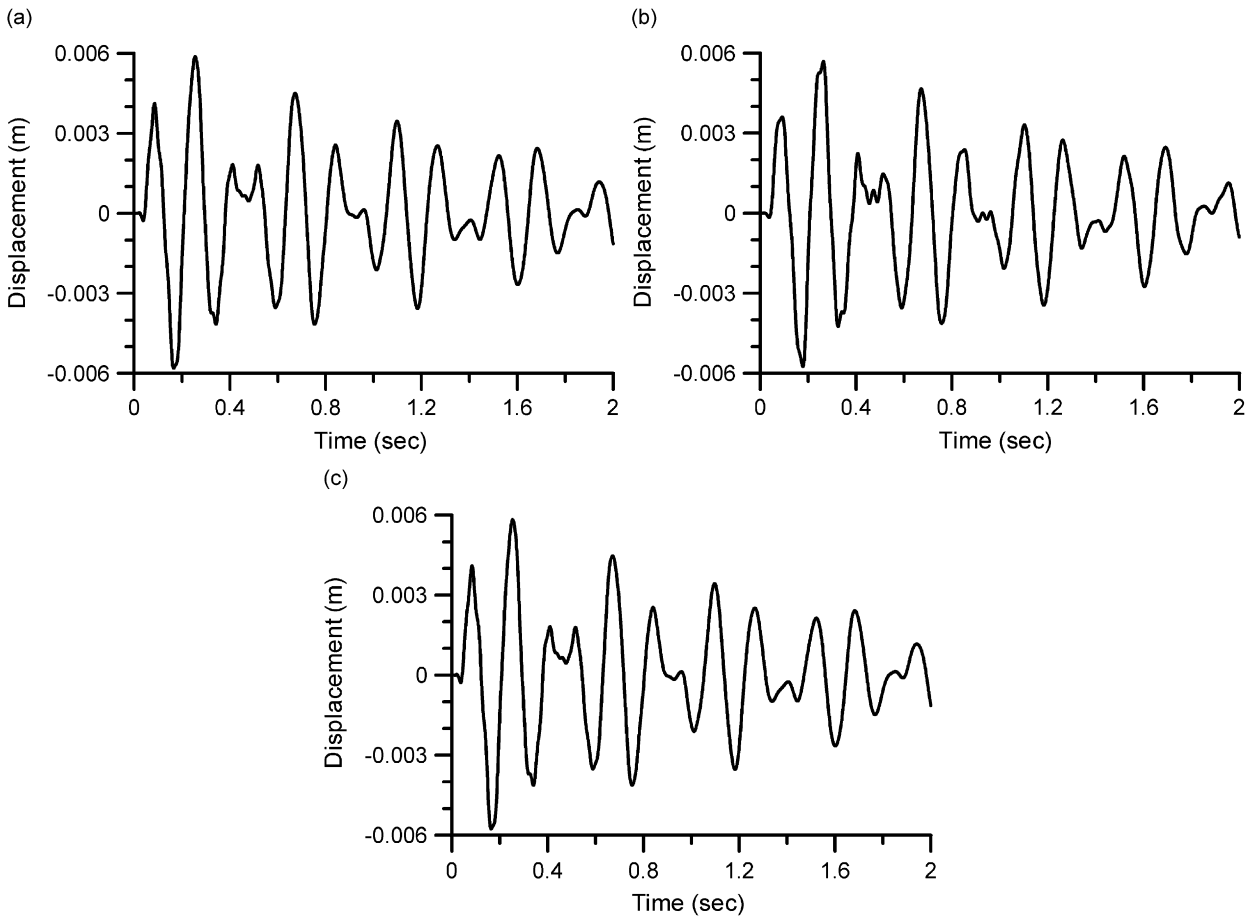

Fig. 8. Vertical displacements at node 6 of cross frame without hinge under 20 Hz vertical force: (a) continuous mass (2 elements per beam); (b) discrete mass (4 elements per beam) and (c) discrete mass (40 elements per beam).

If a hinge is put on the center joint of the frame to limit the translation of the center joint as shown in Fig. 3(b), modes 2–4 become the triple-roots modes and have the same natural frequency of the first flexural pole ω_{b1} as shown in Fig. 5. The corresponding generalized mass terms defined in Eq. (38) are $m_{22}=1.0$, $m_{23}=1.850\times10^{-17}$, $m_{33}=1.0$, $m_{24}=1.157\times10^{-16}$, $m_{34}=3.538\times10^{-17}$, $m_{44}=1.0$, which indicates that the off-diagonal terms m_{nk} in Eq. (37) are negligible, because the three mode shapes are orthogonal. Similarly, modes 6–8 become the triple-roots modes and have the same natural frequency of the second flexural pole ω_{b2}.

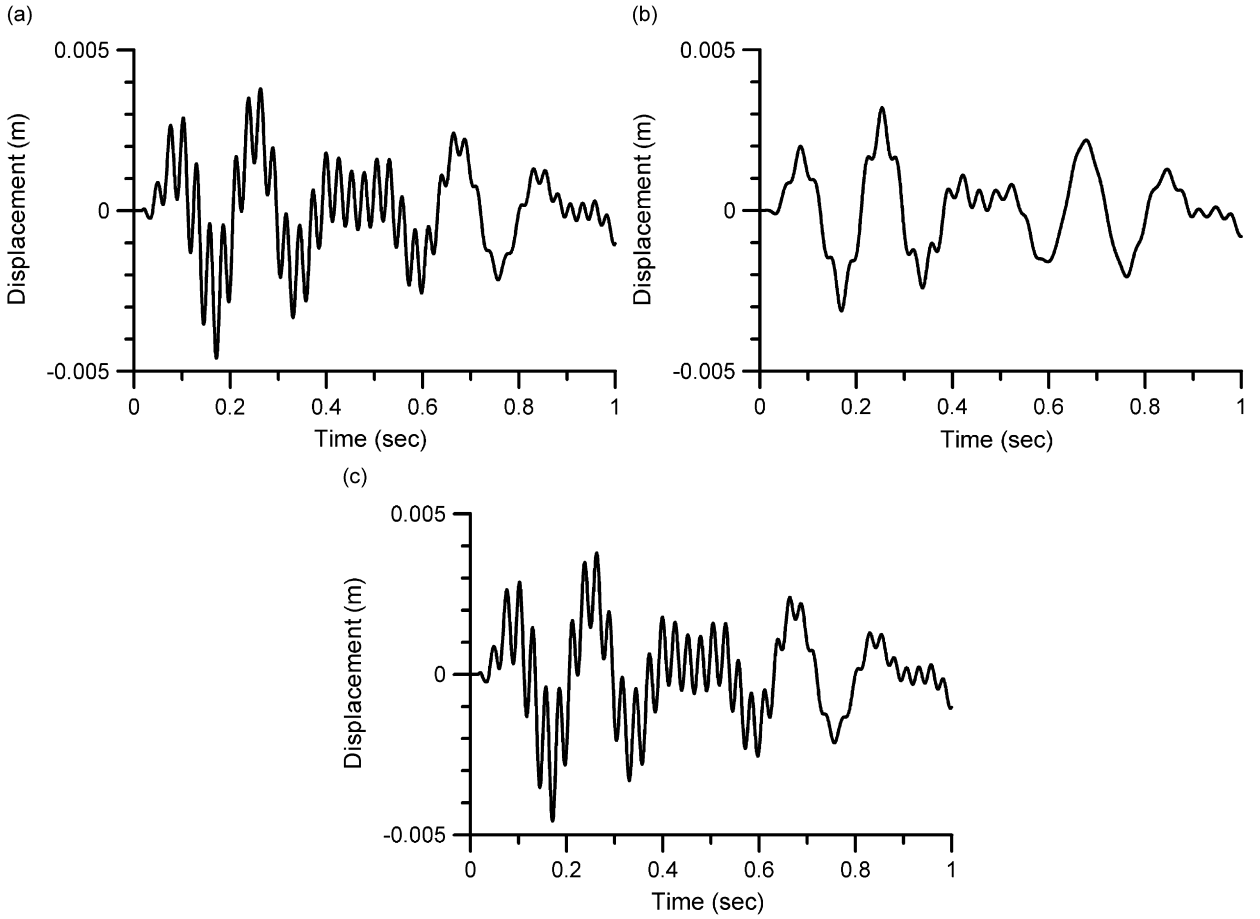

Fig. 9. Vertical displacements at node 6 of cross frame without hinge under 40 Hz vertical force: (a) continuous mass (2 elements per beam); (b) discrete mass (4 elements per beam) and (c) discrete mass (40 elements per beam).

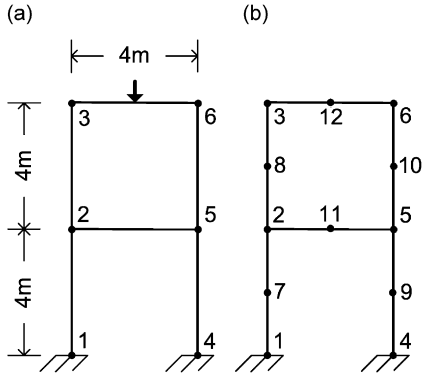

Fig. 10. Two-story frames in example 2: (a) $A=10^{-2}\,m^2$ and (b) $A=10^{4}\,m^2$.

The axial poles of the beams in the cross frames are $\omega_{an}=125n$ Hz, calculated from Eq. (45) with $L=4$ m. For the cross frame without hinge, the null modes of axial poles are double-roots. Plotted in the perpendicular direction of the beam axes, Fig. 6 shows the axial displacements of the modes corresponding to frequencies ω_{a1} and ω_{a2}. Because a middle node has been added to each beam, modes 24 and 25 corresponding to frequency ω_{a1} are not null mode and their mode shape vectors are solved by the procedure described in Section 7. However, modes 39 and 40 corresponding to frequency ω_{a2} are null mode and their mode shape vectors are solved by the procedure described in Section 8. For the cross frame with hinge, the null modes of axial poles are quadruple-roots. Fig. 7 shows the axial displacements of the modes corresponding to frequency ω_{a2}.

To study the effect of distributed mass, a vertical harmonic force $\sin\omega t$ kN is applied at node 2 of the cross frame without hinge. The damping properties of the cross frame are $\zeta=10^{-4}$ and $\eta=1$. The vertical displacement at node 6 is calculated by the distributed-mass approach and the lumped-mass approach. In the lumped-mass approach, every beam is

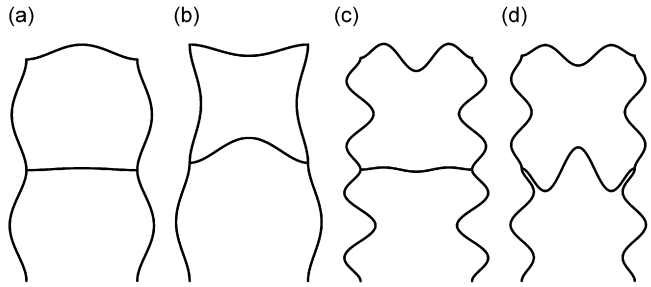

Fig. 11. Mode shapes of two-story frame ($A=10^4$ m^2): (a) mode 6 (7.038 Hz); (b) mode 7 (7.038 Hz); (c) mode 18 (38.03 Hz) and (d) mode 19 (38.03 Hz).

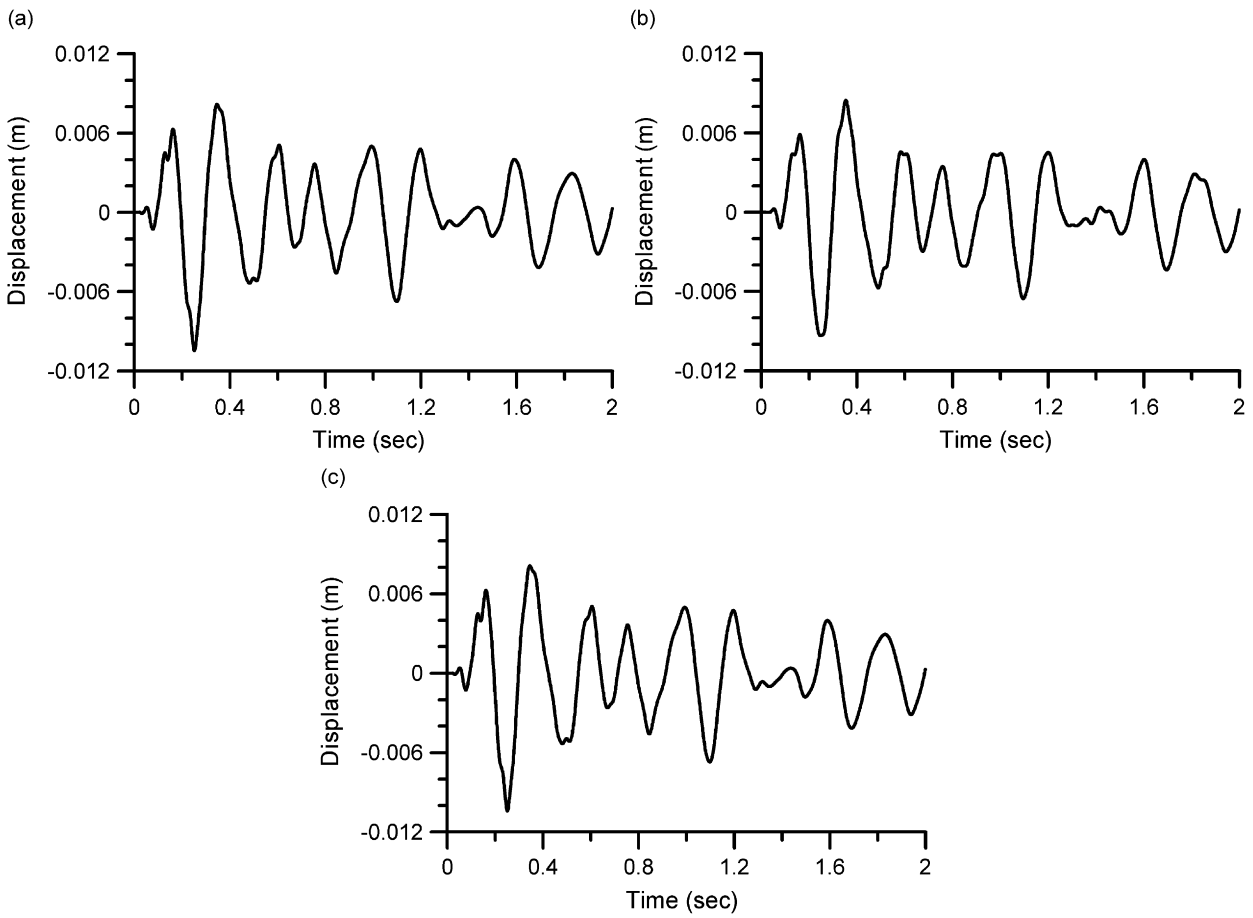

Fig. 12. Vertical displacements at middle of first story in two-story frame ($A=10^{-2}$ m^2) under 20 Hz vertical force: (a) continuous mass (1 element per beam); (b) discrete mass (4 elements per beam) and (c) discrete mass (40 elements per beam).

divided into 4 elements or 40 elements. For the input frequency $\omega=20$ Hz, Fig. 8 reveals that the response calculated by the distributed-mass approach only has some variation in high frequency from the response by the lumped-mass approach using 4 elements per beam, and is the same as the response by the lumped-mass approach using 40 elements per beam. However, if the input frequency ω is increased to 40 Hz, the response calculated by the distributed-mass approach is completely different from the response calculated by the lumped-mass approach using 4 elements per beam as shown in Fig. 9. When every beam is divided into 40 elements, the response by the lumped-mass approach is the same as the response by the distributed-mass approach. For the lumped-mass approach, increasing the number of divided elements in every beam can reduce the response difference from the distributed-mass approach.

9.2. Example 2

The two-story frame shown in Fig. 10(a) consists of six prismatic beams with 4 m length. Every beam has the same properties of $E=10^9$ N/m^2, $\rho=10^3$ kg/m^3, $A=10^{-2}$ m^2 and $I=10^{-5}$ m^4. Modal analysis indicates that the frame does not have any null mode of flexural poles or axial poles. However, if the axial deformation is neglected by increasing the beam area to $A=10^4$ m^2 but keeping the same mass per length, i.e. $\rho A=10$ kg/m, the frame possesses the modes of which the natural frequencies equal to the flexural poles ω_{bn} with $n=1,3,5,\ldots$. The residuals of these mode shapes are very high, which indicates that the frame needs additional middle nodes for every beam, as shown in Fig. 10(b), to eliminate the null modes of flexural poles. Fig. 11 depicts the shapes of modes 6 and 7 which have the same frequency as $\omega_{b1}=7.038$ Hz and the shapes of modes 18 and 19 which have the same frequency as $\omega_{b3}=38.03$ Hz.

The frame of Fig. 10(a) is subjected to a vertical harmonic force $\sin\omega t$ kN at the center of the second story. The damping properties of the frame are $\zeta=10^{-4}$ and $\eta=1$. The histories of the vertical displacement at the middle of the first story for the input frequency $\omega=20$ Hz, plotted in Fig. 12, reveals that the distributed-mass approach has a slight difference from the lumped-mass approach using 4 elements per beam, and is the same as the lumped-mass approach using 40 elements per beam. The curves in Fig. 13 are the responses excited by the input frequency $\omega=40$ Hz and show a difference between the

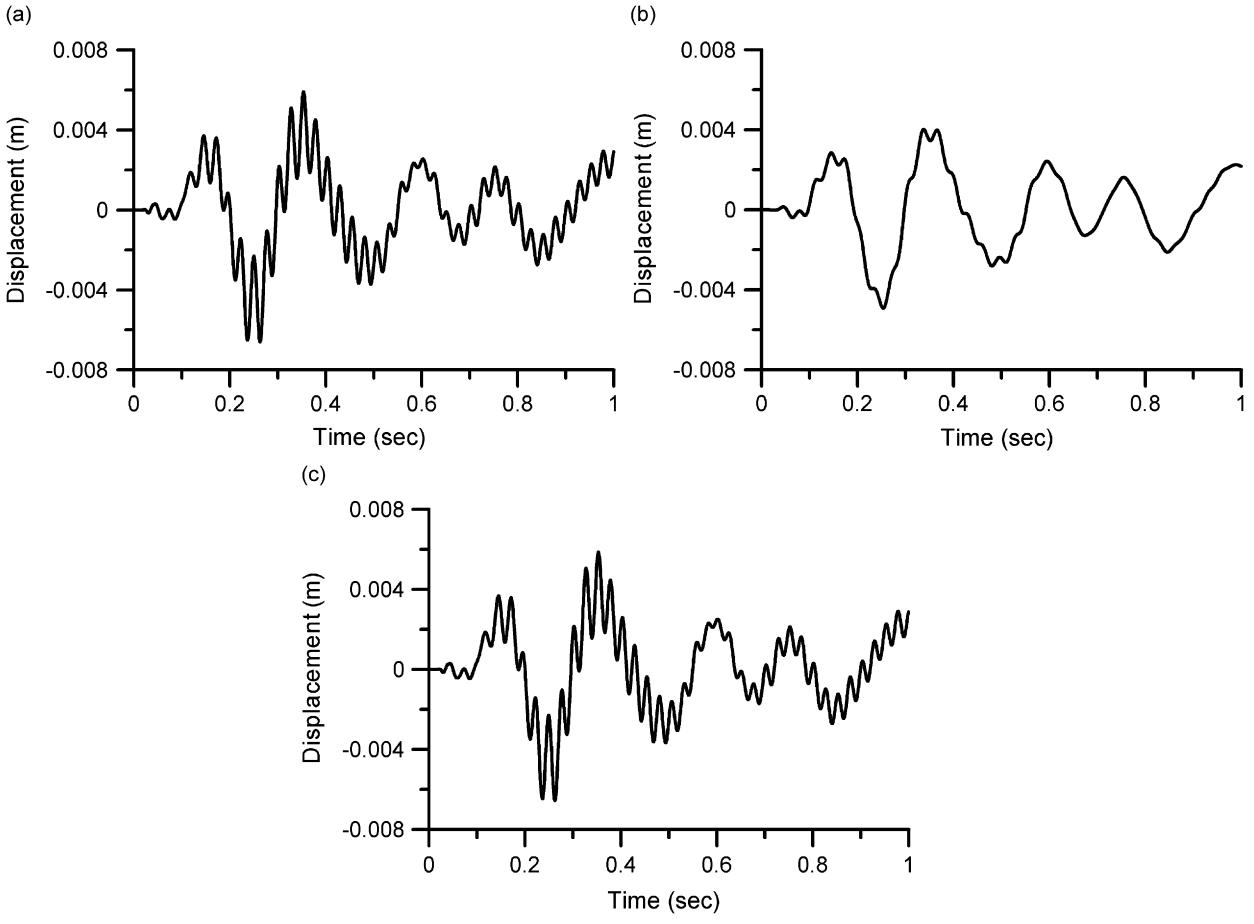

Fig. 13. Vertical displacements at middle of first story in two-story frame ($A=10^{-2}$ m^2) under 40 Hz vertical force: (a) continuous mass (1 element per beam); (b) discrete mass (4 elements per beam) and (c) discrete mass (40 elements per beam).

distributed-mass approach and the lumped-mass approach using 4 elements per beam. The response calculated by the lumped-mass approach using 40 elements per beam is the same as the response calculated by the distributed-mass approach.

10. Conclusion

The dynamic stiffness method is the exact method for the dynamic analysis of plane frames including the effect of mass distribution in beam elements. Derived from the vibration theory of Bernoulli–Euler beams and including axial deformation, the dynamic stiffness matrices of beam elements can be robotically assembled to form the dynamic stiffness of the plane frame from which the natural frequencies of the frames can be accurately determined by the Wittrick–Williams algorithm. The mode shapes can be found using the deflated dynamic stiffness matrix. If the residual of the solved mode shape is too high to be accepted, iteration with seeking the new deflated location may be required. For the modes of repeated roots, the process of Gram–Schmidt orthogonalization can generate the orthogonal mode shapes that span the vector space of repeated-root modes. The deflated matrix approach for the mode shapes cannot be applied to the null modes where the deformations at all frame joints are null but the deformations in beam elements are not null. If the null modes have the flexural deformation in beam elements, adding a middle node to every beam element of the frame can normalize these modes, i.e., become non-null. However, the null modes having the axial deformation in beam elements cannot be completely normalized by adding nodes to beam elements, but their axial deformation can be calculated by using the approach of nodal force equilibrium to find the amplitude of axial force in beam elements.

Orthogonal properties of vibration modes in the Bernoulli–Euler plane frames considering distributed mass have been theoretically derived, through which the equations of motion in beam elements can be transformed into the decoupled equations of motion in terms of mode amplitudes. After solving for the transient response of each vibration mode from the decoupled equations of motion, the frame deformation and element stresses can be calculated by the mode superposition approach.

Acknowledgments

The National Science Council of Taiwan supported the research work reported in this paper under Grant no. NSC97-2211-E011-068. This support is greatly appreciated.

References

[1] R.R. Craig, Jr, *Structural Dynamics*, Wiley, New York, 1981.
[2] A.K. Chopra, *Dynamics of Structures*, second ed., Prentice-Hall, New York, 1995.
[3] M. Paz, Mathematical observations in structural dynamics, *Computers and Structures* 3 (1973) 385–396.
[4] B.A. Akesson, PFVIBAT—a computer program for plane frame vibration analysis by an exact method, *International Journal for Numerical Methods in Engineering* 10 (1976) 1221–1231.
[5] F.W. Williams, W.H. Wittrick, An automatic computational procedure for calculating natural frequencies of skeletal structures, *International Journal of Mechanical Sciences* 12 (1970) 781–791.
[6] W.H. Wittrick, F.W. Williams, A general algorithm for computing natural frequencies of elastic structures, *Quarterly Journal of Mechanics and Applied Mathematics* 24 (1971) 263–284.
[7] D. Kennedy, F.W. Williams, More efficient use of determinants to solve transcendental structural eigenvalue problems reliably, *Computers and Structures* 41 (1991) 973–979.
[8] K.L. Chan, F.W. Williams, Orthogonality of modes of structures when using the exact transcendental stiffness matrix method, *Shock and Vibration* 7 (2000) 23–28.
[9] C.T. Hopper, F.W. Williams, Mode finding in nonlinear structural eigenvalue calculations, *Journal of Structural Mechanics* 5 (1977) 255–278.
[10] S. Yuan, K. Ye, F.W. Williams, Second order mode-finding method in dynamic stiffness matrix method, *Journal of Sound and Vibration* 269 (2004) 689–708.
[11] C.A.N. Dias, M. Alves, A contribution to the exact modal solution of in-plane beam structures, *Journal of Sound and Vibration* 328 (2009) 586–606.